

NEW FORMULATION FOR COMPOSITE SANDWICH SHELL FINITE ELEMENT

Romil Tanov* and Ala Tabiei†

Center of Excellence in DYNA3D Analysis
Department of Aerospace Engineering and Engineering Mechanics
University of Cincinnati, OH 45221-0070, USA

ABSTRACT

A new homogenization procedure for Finite Element (FE) analysis of sandwich shells was recently developed and presented by the authors. To the authors' knowledge all present FE approaches to sandwich structures are incorporated into the FE formulation on the element formulation level. Unlike other formulations the present approach works on the constitutive level. A homogenization of the sandwich shell is performed at each call of the corresponding constitutive subroutine. Thus the sandwich nature of the problem is hidden from the main FE program. As a consequence there is no need to develop a new shell element formulation, but instead all available homogeneous shell elements in the utilized FE code can be used for the analysis of sandwich shells. This would provide versatility of the FE analysis and potentials to trade off between the level of accuracy and computational efficiency by using more accurate or simpler shell elements. Furthermore, the sandwich homogenization procedure (SHOP) can be easily coupled with a composite homogenization model to enable analysis of sandwich shells with composite faces. To validate the present approach and check its accuracy, efficiency and overall performance it is implemented in a finite element package and combined with existing first order shear deformable shell elements for homogeneous materials. Results are obtained and herein presented for problems previously investigated experimentally and by different theoretical and numerical techniques. The presented results show good agreement with published results from far more complicated and computationally intensive analyses, which builds confidence in the approach and motives its future elaboration and development.

Keywords: sandwich shells, finite element analysis, sandwich homogenization, shell elements, composite faces, plate deformations

INTRODUCTION

As the technological, structural, thermal, acoustic, durability, and other requirements for shell structures increase so does the application of sandwich panels in land, marine, space vehicles, civil structures etc. While in some cases the design requirements could still be satisfied by using conventional construction materials like metals and the application of sandwich shells is simply a matter of choice, recently there are more and more areas where conventional materials simply won't do the job. Structural, thermal etc. characteristics have to be tailored and combined, and therefore, in such cases the utilization of sandwich constructions is inevitable. Their important advantages like high weight to stiffness and weight to strength

* Graduate Res. Assistant

† Assist. Prof. and Director, author to whom correspondence should be addressed

ratios and durability would have increased their application even more if it were not for the technological difficulties related to their production, high cost per unit volume, and the uncertainty in predicting their behavior. The structural complexity of sandwich shells makes standard analysis methods developed for homogeneous shells inapplicable and the results acquired with them are usually inaccurate and unreliable. Therefore, major efforts are devoted to developing analysis tools capable of adequately predicting the behavior of sandwich shells. A significant part of these efforts is dedicated to the utilization of the FE analysis for predicting the behavior of sandwich shells.

The basic difference between sandwich and homogeneous shells is the significant contribution of the transverse shear to the shell deformation. Furthermore, some derivatives of the displacement functions are discontinuous through the shell thickness. All this makes classic shell theories based on Love-Kirchhoff hypotheses inapplicable for sandwich shell analysis. In the FE formulation for shell structures the utilized shell theory is implemented on the element formulation level. Therefore, it is not surprising that most of the efforts in applying the FE method for sandwich shells investigation are concentrated on the element formulation level. Probably the easiest approach is just to use 3-D finite elements and separately discretize the different sandwich layers – faces and core. In most cases this will provide good accuracy but results in a very fine FE mesh and is only applicable for small models and simple problems. In an effort to improve the analysis efficiency most of the developed approaches rely on some a priori assumed through thickness distribution for the unknowns: displacements, strains and stresses. Thus, a reduction in the problem dimensionality is done, which is supposed to result in a significant decrease in the number of degrees of freedom of the system. In this process the usual controversy in engineering analysis appears, having to trade off between efficiency and accuracy. The simplest approaches are usually not accurate enough and the accurate ones are not efficient enough to be applicable for real world problems.

First Order Shear Deformable Theories

The simplest approaches are based on the single layer assumption: the shell is assumed made of an equivalent single homogeneous layer. In this theory the discontinuities of displacement derivatives at the face-core interfaces are neglected. These discontinuities are taken into account by the more complex layered approaches. Most of the earliest developed approaches to sandwich shell analysis are based on the Reissner-Mindlin (see Reissner¹ and Mindlin²) type first order shear deformation theories and utilize the single layer assumption. These theories assume that sections, which are initially plane and perpendicular to the reference surface, remain plane but are not necessarily normal to the reference surface after the loading is applied. Hrabok and Hruby³, Ha⁴, Burton and Noor⁵, Zenkert⁶, and the extensive review by Noor et al⁷ have described and referenced many of these theories. The major disadvantage of the first order theories is that they cannot correctly represent the through thickness distribution of the transverse shear deformation. As a result the traction conditions at the shell surfaces are violated and as the shell thickness decreases these theories tend to experience shear locking. They require shear correction coefficients to correct the corresponding strain energy terms and these coefficients are not always available or easy to determine.

Higher Order Theories

To overcome some of the disadvantages of the first order theories the through thickness distributions of the displacement functions are assumed to be higher order polynomials of the thickness coordinate. Quadratic, cubic, or higher polynomials have been assumed by different authors. Higher order theories have been systematically described and referenced by Pandya and Kant⁸, Reddy⁹, Ha⁴, and Noor et al⁷. The basic disadvantage of the higher order theories is that most of them require C^1 continuity of the displacements. To overcome this Kant and Kommineni¹⁰ developed a C^0 formulation of a higher order shear deformation theory.

Discrete Layer and Zig-Zag Theories

To overcome the violation of the strain and stress discontinuities through the shell thickness of the first and higher order single layer theories discrete layer and zig-zag theories have been developed. The discrete layer theories,¹¹⁻¹⁵ assume that the sandwich shell is composed of layers of different materials with different distribution of the displacements in the separate layers. This approach is applied both for composite and sandwich shells. For sandwich shells the faces and core are usually defined as separate layers. These theories usually result in quite accurate representation of the sandwich shell behavior but a major disadvantage is that they require a large number of degrees of freedom to be able to represent the through thickness displacement functions. This significantly affects the computational efficiency making them suitable only for small problems. Zig-zag theories,¹⁶⁻¹⁹ usually require a smaller number of degrees of freedom but still give a good representation of the continuity and traction conditions at layer interfaces. Some of these theories,^{18, 19} are based on C^0 elements and seem efficient for layered composite and sandwich shells.

The Sandwich Homogenization Procedure (SHOP)

The aim of the present approach is to use the simplicity of the single layer approach and yet keep the layered nature of the shell. Within the FE analysis this is done by performing a homogenization of the sandwich layers on the constitutive level. Stresses in the faces and core, which correspond to the incoming strains, are computed, homogenized and returned to the FE subroutine for calculation of internal forces. Thus, the sandwich nature of the shell is only manifested on the material constitutive level. It is hidden from the main FE program, which means that practically no changes to the existing code are necessary outside of the shell through thickness integration loop.

By using the single layer approach the SHOP inherits its disadvantage: representing each of the through thickness displacements and their derivatives by a single continuous function with continuous derivatives. In the actual sandwich shell the displacements themselves are continuous but some of their derivatives are discontinuous, which results in some discontinuities in the strain functions. For the continuous displacements and strains a formulation involving a higher order single layer theory will probably give a sufficiently accurate approximation of the corresponding displacements and strains. Using first order shell elements, the present implementation of the SHOP yields very good results for the normal strains in sections where no excessive warping is observed. To deal with the discontinuities in the transverse shear strains, the present procedure changes the strain distribution through the thickness. This change is based on the shear stresses interface traction conditions, and it results in a more realistic transverse strain distribution functions. As seen from the presented graphs, the results produced by the SHOP are very reasonable.

THE SHOP AND ITS PRESENT IMPLEMENTATION

Description of the SHOP

The proposed SHOP performs the standard task of any finite element material model: receiving the strain increments in the equivalent material it calculates the corresponding stress increments. For this homogenization procedure to work it is necessary to process all integration points throughout a given cross section simultaneously. This is due to the fact that the sandwich nature of the problem is hidden from the main program and is only considered within the homogenization procedure. Based on assumptions relating the equivalent homogeneous shell and the sandwich shell, the stress increments in the sandwich and in the equivalent material cross section are calculated from the strain increment distribution in the equivalent material cross section. The assumptions that the SHOP is based upon are:

- ♦ *The strain increment distribution functions throughout the cross-section of the equivalent material are known.*
- ♦ *The faces and core layers of the sandwich shell and the equivalent shell material are assumed homogeneous and orthotropic.*
- ♦ *The “equivalence” between the fictitious equivalent shell and the sandwich shell is based on assumed equalities of the cross-sectional resultant forces and moments, and the strain energy for the cross section;*
- ♦ *Although the proposed material model can be developed for unsymmetrical sandwich shells, in the present study a symmetric sandwich shell is assumed. Both faces have the same thickness, h_f , and are of the same material. The thickness of the core is denoted with h_c .*

The formulation of the proposed homogenization procedure is rather simple. It receives from the finite element main program the values of the strain increments at the integration points of the current cross section. Knowing the shell formulation that the current shell element is based upon, the strain increment distribution functions throughout the shell cross section can be determined. Assuming the same distribution and the same values for the strains in the sandwich shell cross section and based on the known material constitutive relations, the stress distribution and corresponding values in the faces and core layers can be calculated. The resultant forces and moments for the cross section can also be calculated. Assuming that the stress increments in the equivalent material produce the same values for the resultant forces and moments, they can be expressed through the strain increment distribution functions and the unknown constitutive relation constants of the equivalent material. From these expressions the unknown constitutive constants of the equivalent material can be determined and with them the stress increments in the equivalent material integration points can be calculated. This approach should be able to work with single layer shell theories of any order.

Implementation of the SHOP

In the present investigation the SHOP is incorporated in an existing FE package and is combined with standard first order shell elements. The linear strain and stress distribution through the shell thickness allows for some simplifications in the formulation: instead of the equivalent material constitutive constants the equivalent material stresses in the integration points can be directly calculated. Furthermore, the constant transverse shear assumption allows the transverse shear strain distribution in the sandwich shell to be changed satisfying the shear stress interface requirements. The basic homogenization assumptions of the SHOP involve equalities between the cross-sectional resultant forces and moments for the sandwich shell and the equivalent homogeneous shell. Equality is assumed between the following resultant forces and moments:

- N_{xx} – the resultant force of stress increments $d\sigma_{xx}$ for the cross-section with normal the x -axis;
- N_{yy} – the resultant force of stress increments $d\sigma_{yy}$ for the cross-section with normal the y -axis;
- $N_{xy} = N_{yx}$ – the resultant shear force of stress increments $d\sigma_{xy} = d\sigma_{yx}$ in the shell plane;
- M_{xx} – the resultant moment of the stress increments $d\sigma_{xx}$ about the y -axis;
- M_{yy} – the resultant moment of the stress increments $d\sigma_{yy}$ about the x -axis;
- $M_{xy} = M_{yx}$ – the resultant moment of the stress increments $d\sigma_{xy}$ about the x -axis, or of $d\sigma_{yx}$ about the y -axis.

The developed procedure utilizes the [Hughes et al, 20] degenerate shell element. Three integration points through the thickness are considered. One at the mid-surface and two above and below the mid surface. Faces and core materials are assumed to be orthotropic. The incremental strains are related to the incremental stresses for both faces and core by the compliance and stiffness matrices given by equations (1 and 2).

$$\begin{Bmatrix} d\boldsymbol{\varepsilon}_{xx}^k \\ d\boldsymbol{\varepsilon}_{yy}^k \\ d\boldsymbol{\varepsilon}_{zz}^k \\ d\boldsymbol{\varepsilon}_{xy}^k \\ d\boldsymbol{\varepsilon}_{yz}^k \\ d\boldsymbol{\varepsilon}_{zx}^k \end{Bmatrix} = \begin{bmatrix} \frac{1}{E_{11}^k} & -\nu_{21}^k & -\nu_{31}^k & 0 & 0 & 0 \\ \frac{-\nu_{12}^k}{E_{11}^k} & \frac{1}{E_{22}^k} & -\nu_{32}^k & 0 & 0 & 0 \\ \frac{-\nu_{13}^k}{E_{11}^k} & \frac{-\nu_{23}^k}{E_{22}^k} & \frac{1}{E_{33}^k} & 0 & 0 & 0 \\ 0 & 0 & 0 & \frac{1}{G_{12}^k} & 0 & 0 \\ 0 & 0 & 0 & 0 & \frac{1}{G_{23}^k} & 0 \\ 0 & 0 & 0 & 0 & 0 & \frac{1}{G_{31}^k} \end{bmatrix} \begin{Bmatrix} d\boldsymbol{\sigma}_{xx}^k \\ d\boldsymbol{\sigma}_{yy}^k \\ d\boldsymbol{\sigma}_{zz}^k \\ d\boldsymbol{\sigma}_{xy}^k \\ d\boldsymbol{\sigma}_{yz}^k \\ d\boldsymbol{\sigma}_{zx}^k \end{Bmatrix} \quad (1)$$

where k is f, c for face or core, respectively

$$\begin{Bmatrix} d\boldsymbol{\sigma}_{xx}^k \\ d\boldsymbol{\sigma}_{yy}^k \\ d\boldsymbol{\sigma}_{zz}^k \\ d\boldsymbol{\sigma}_{xy}^k \\ d\boldsymbol{\sigma}_{yz}^k \\ d\boldsymbol{\sigma}_{zx}^k \end{Bmatrix} = \begin{bmatrix} C_{11}^k & C_{12}^k & C_{13}^k & 0 & 0 & 0 \\ C_{12}^k & C_{22}^k & C_{23}^k & 0 & 0 & 0 \\ C_{13}^k & C_{23}^k & C_{33}^k & 0 & 0 & 0 \\ 0 & 0 & 0 & C_{44}^k & 0 & 0 \\ 0 & 0 & 0 & 0 & C_{55}^k & 0 \\ 0 & 0 & 0 & 0 & 0 & C_{66}^k \end{bmatrix} \begin{Bmatrix} d\boldsymbol{\varepsilon}_{xx}^k \\ d\boldsymbol{\varepsilon}_{yy}^k \\ d\boldsymbol{\varepsilon}_{zz}^k \\ d\boldsymbol{\varepsilon}_{xy}^k \\ d\boldsymbol{\varepsilon}_{yz}^k \\ d\boldsymbol{\varepsilon}_{zx}^k \end{Bmatrix} \quad (2)$$

where k is f, c, e for face, core, or equivalent material respectively.

The nonlinear finite element code DYNA3D is considered for implementation of the present formulation. The strains at the three integration points are obtained after kinematic updates. These strains are cascaded to the faces and core to calculate the stresses. Once stresses in faces and core are calculated, equivalence of moment and stress resultants is invoked to obtain the stresses of the equivalent shell at the three integration points. These stresses are then used to calculate the internal forces in the shell element and to subsequently obtain strains at the next increment. Membrane and bending strains at the three integration points are used to calculate stress and moment resultants. The Hughes shell element assumes that the transverse normal stress vanishes (equation 3), however, the formulation allows for non-zero transverse normal strain at the nodal points. The transverse normal strain in the faces and core due to membrane strains are given by the following equations:

$$d\boldsymbol{\sigma}_{zz}^e = d\boldsymbol{\sigma}_{zz}^f = d\boldsymbol{\sigma}_{zz}^c = 0 \quad (3)$$

$$d\boldsymbol{\varepsilon}_{zz}^f = -\frac{C_{13}^f d\boldsymbol{\varepsilon}_{xx}(0) + C_{23}^f d\boldsymbol{\varepsilon}_{yy}(0)}{C_{33}^f} \quad (4)$$

$$d\boldsymbol{\varepsilon}_{zz}^c = -\frac{-C_{13}^c d\boldsymbol{\varepsilon}_{xx}(0) + C_{23}^c d\boldsymbol{\varepsilon}_{yy}(0)}{C_{33}^c}$$

Stresses Due to Stretching:

Label the integration point at the mid-surface as integration point one and the integration points above and below the mid-surface as integration points 2 and 3 respectively as depicted by Figure (1). At the mid-surface integration point ($z=0$) the membrane strains are given by the following equations:

$$\begin{aligned} d\boldsymbol{\varepsilon}_{xx}(0) &= e_1(1) \\ d\boldsymbol{\varepsilon}_{yy}(0) &= e_2(1) \\ d\boldsymbol{\varepsilon}_{xy}(0) &= e_4(1) \end{aligned} \quad (5)$$

where $e_i(1)$ are the strains at mid-section integration point, and $i=1, 2,$ and 4 respectively.

Due to these strains, the membrane strains in the faces and core are calculated as follows:

Face

$$\begin{aligned} d\boldsymbol{\sigma}_{xx}^f(0) &= C_{11}^f e_1(1) + C_{12}^f e_2(1) + C_{13}^f d\boldsymbol{\varepsilon}_{zz}^f(0) \\ d\boldsymbol{\sigma}_{yy}^f(0) &= C_{12}^f e_1(1) + C_{22}^f e_2(1) + C_{23}^f d\boldsymbol{\varepsilon}_{zz}^f(0) \\ d\boldsymbol{\sigma}_{xy}^f(0) &= C_{44}^f(0) e_4(1) \end{aligned} \quad (6)$$

Core

$$\begin{aligned} d\boldsymbol{\sigma}_{xx}^c(0) &= C_{11}^c e_1(1) + C_{12}^c e_2(1) + C_{13}^c d\boldsymbol{\varepsilon}_{zz}^c(0) \\ d\boldsymbol{\sigma}_{yy}^c(0) &= C_{12}^c e_1(1) + C_{22}^c e_2(1) + C_{23}^c d\boldsymbol{\varepsilon}_{zz}^c(0) \\ d\boldsymbol{\sigma}_{xy}^c(0) &= C_{44}^c e_4(1) \end{aligned} \quad (7)$$

The stress resultants due to the membrane stretching are calculated by the following equations:

$$\begin{aligned} N_{xx} &= 2h_f d\boldsymbol{\sigma}_{xx}^f(0) + h_c d\boldsymbol{\sigma}_{xx}^c(0) \\ N_{yy} &= 2h_f d\boldsymbol{\sigma}_{yy}^f(0) + h_c d\boldsymbol{\sigma}_{yy}^c(0) \\ N_{xy} &= 2h_f d\boldsymbol{\sigma}_{xy}^f(0) + h_c d\boldsymbol{\sigma}_{xy}^c(0) \end{aligned} \quad (8)$$

where h_f, h_c is the thickness of the faces and core respectively.

Stresses Due to Bending:

Stresses due to bending deformation are calculated from the increments of the cross-section rotations given by the following equations:

$$\begin{aligned} \theta_x &= \frac{e_1(2) - e_1(1)}{eta} \\ \theta_y &= \frac{e_2(2) - e_2(1)}{eta} \\ \theta_{xy} &= \frac{e_4(2) - e_4(1)}{eta} \end{aligned} \quad (9)$$

where $e_i(2)$: are strains at second integration point above mid-surface and $i=1, 2,$ and 4 respectively and eta : is the distance between the integration points as depicted in Figure (2). Once the incremental cross-section rotations are obtained, the incremental strains due to the bending deformation are calculated in the faces and core. The incremental stresses due to

bending are calculated using the constitutive equations of the face and core respectively. Subsequently the moment resultants in both faces and core are obtained. The corresponding equations are as follows:

Face at $z = -\frac{h_t}{2}$

The incremental bending strains in the face due to cross-section rotations are:

$$\begin{aligned} d\varepsilon_{xx}\left(-\frac{h_t}{2}\right) &= -\theta_x \frac{h_t}{2} \\ d\varepsilon_{yy}\left(-\frac{h_t}{2}\right) &= -\theta_y \frac{h_t}{2} \\ d\varepsilon_{xy}\left(-\frac{h_t}{2}\right) &= -\theta_{xy} \frac{h_t}{2} \end{aligned} \quad (10)$$

and

$$d\varepsilon_{zz}\left(-\frac{h_t}{2}\right) = \frac{C_{13}^f \theta_x + C_{23}^f \theta_y}{C_{33}^f} \frac{h_t}{2}$$

The incremental bending stresses due to cross-section rotations are:

$$\begin{aligned} d\sigma_{xx}^f\left(-\frac{h_t}{2}\right) &= \frac{h_t}{2} \left[-C_{11}^f \theta_x - C_{12}^f \theta_y + C_{13}^f \left(\frac{C_{13}^f \theta_x + C_{23}^f \theta_y}{C_{33}^f} \right) \right] \\ d\sigma_{yy}^f\left(-\frac{h_t}{2}\right) &= \frac{h_t}{2} \left[-C_{12}^f \theta_x - C_{22}^f \theta_y + C_{23}^f \left(\frac{C_{13}^f \theta_x + C_{23}^f \theta_y}{C_{33}^f} \right) \right] \\ d\sigma_{xy}^f\left(-\frac{h_t}{2}\right) &= -\frac{h_t}{2} C_{44}^f \theta_{xy} \end{aligned} \quad (11)$$

Therefore the moment resultants in faces can be obtained from the following equations:

$$\begin{aligned} M_{xx}^f &= \frac{d\sigma_{xx}^f\left(-\frac{h_t}{2}\right)}{6h_t} (h_t^3 - h_c^3) \\ M_{yy}^f &= \frac{d\sigma_{yy}^f\left(-\frac{h_t}{2}\right)}{6h_t} (h_t^3 - h_c^3) \\ M_{xy}^f &= \frac{d\sigma_{xy}^f\left(-\frac{h_t}{2}\right)}{6h_t} (h_t^3 - h_c^3) \end{aligned} \quad (12)$$

In the above equations $h_t = 2h_f + h_c$.

Core at $z = -\frac{h_c}{2}$

The incremental bending strains in the core due to cross-section rotations are:

$$\begin{aligned}
d\boldsymbol{\varepsilon}_{xx}^c\left(-\frac{h_c}{2}\right) &= -\boldsymbol{\theta}_x \frac{h_c}{2} \\
d\boldsymbol{\varepsilon}_{yy}^c\left(-\frac{h_c}{2}\right) &= -\boldsymbol{\theta}_y \frac{h_c}{2} \\
d\boldsymbol{\varepsilon}_{xy}^c\left(-\frac{h_c}{2}\right) &= -\boldsymbol{\theta}_{xy} \frac{h_c}{2}
\end{aligned} \tag{13}$$

and

$$d\boldsymbol{\varepsilon}_{zz}^c\left(-\frac{h_c}{2}\right) = \frac{C_{13}^c \boldsymbol{\theta}_x + C_{23}^c \boldsymbol{\theta}_y}{C_{33}^c} \frac{h_c}{2}$$

The incremental bending stresses due to cross-section rotations are:

$$\begin{aligned}
d\boldsymbol{\sigma}_{xx}^c\left(-\frac{h_c}{2}\right) &= \frac{h_c}{2} \left[-C_{11}^c \boldsymbol{\theta}_x - C_{12}^c \boldsymbol{\theta}_y + C_{13}^c \left(\frac{C_{13}^c \boldsymbol{\theta}_x + C_{23}^c \boldsymbol{\theta}_y}{C_{33}^c} \right) \right] \\
d\boldsymbol{\sigma}_{yy}^c\left(-\frac{h_c}{2}\right) &= \frac{h_c}{2} \left[-C_{12}^c \boldsymbol{\theta}_x - C_{22}^c \boldsymbol{\theta}_y + C_{23}^c \left(\frac{C_{13}^c \boldsymbol{\theta}_x + C_{23}^c \boldsymbol{\theta}_y}{C_{33}^c} \right) \right] \\
d\boldsymbol{\sigma}_{xy}^c\left(-\frac{h_c}{2}\right) &= -\frac{h_c}{2} C_{44}^c \boldsymbol{\theta}_{xy}
\end{aligned} \tag{14}$$

Therefore the moment resultants in the core can be obtained from the following equations:

$$\begin{aligned}
M_{xx}^c &= \frac{h_c^2}{6} d\boldsymbol{\sigma}_{xx}^c\left(-\frac{h_c}{2}\right) \\
M_{yy}^c &= \frac{h_c^2}{6} d\boldsymbol{\sigma}_{yy}^c\left(-\frac{h_c}{2}\right) \\
M_{xy}^c &= \frac{h_c^2}{6} d\boldsymbol{\sigma}_{xy}^c\left(-\frac{h_c}{2}\right)
\end{aligned} \tag{15}$$

The total moment resultants due to bending deformation are obtained as follows:

$$\begin{aligned}
M_{xx} &= M_{xx}^f + M_{xx}^c \\
M_{yy} &= M_{yy}^f + M_{yy}^c \\
M_{xy} &= M_{xy}^f + M_{xy}^c
\end{aligned} \tag{16}$$

Up to this point what we have is the stress and moment resultants in the sandwich shell materials. As stated before, the bases of the formulation is the equivalence of the stress and moment resultants of the sandwich shell and the equivalent homogenized shell. Therefore, the in-plane stresses in the equivalent homogenized shell can be written in the following form at the three integration points of the section:

At the mid-surface integration point:

$$\begin{aligned}
d\sigma_{xx}^e(0) &= \frac{N_{xx}}{h_t} \\
d\sigma_{yy}^e(0) &= \frac{N_{yy}}{h_t} \\
d\sigma_{xy}^e(0) &= \frac{N_{xy}}{h_t}
\end{aligned} \tag{17}$$

At the integration point above the mid-surface

$$\begin{aligned}
d\sigma_{xx}^e(eta) &= d\sigma_{xx}^e(0) - d\sigma_{xx}^{eb}(-eta) \\
d\sigma_{yy}^e(eta) &= d\sigma_{yy}^e(0) - d\sigma_{yy}^{eb}(-eta) \\
d\sigma_{xy}^e(eta) &= d\sigma_{xy}^e(0) - d\sigma_{xy}^{eb}(-eta)
\end{aligned} \tag{18}$$

At the integration point below the mid-surface

$$\begin{aligned}
d\sigma_{xx}^e(-eta) &= d\sigma_{xx}^e(0) + d\sigma_{xx}^{eb}(-eta) \\
d\sigma_{yy}^e(-eta) &= d\sigma_{yy}^e(0) + d\sigma_{yy}^{eb}(-eta) \\
d\sigma_{xy}^e(-eta) &= d\sigma_{xy}^e(0) + d\sigma_{xy}^{eb}(-eta)
\end{aligned} \tag{19}$$

where $d\sigma_{ij}^{eb}(-eta)$ are contributions of the moment resultants and are given by the following:

$$\begin{aligned}
d\sigma_{xx}^{eb}(-eta) &= -\frac{12M_{xx} \times eta}{h_t^3} \\
d\sigma_{yy}^{eb}(-eta) &= -\frac{12M_{yy} \times eta}{h_t^3} \\
d\sigma_{xy}^{eb}(-eta) &= -\frac{12M_{xy} \times eta}{h_t^3}
\end{aligned} \tag{20}$$

The above equations (20) are obtained with the help of Figure (2), and the identity formula for similar triangles. In this manner we have all the in-plane stresses in the equivalent homogenized shell. The normal transverse stress is $d\sigma_{zz}^e = 0$. The transverse shear stresses are obtained from the condition of continuity given by the following equations:

$$\begin{aligned}
d\sigma_{yz}^c &= d\sigma_{yz}^f = d\sigma_{yz}^e \Rightarrow C_{55}^c d\epsilon_{yz}^c = C_{55}^f d\epsilon_{yz}^f \\
d\sigma_{xz}^c &= d\sigma_{xz}^f = d\sigma_{xz}^e \Rightarrow C_{66}^c d\epsilon_{xz}^c = C_{66}^f d\epsilon_{xz}^f
\end{aligned} \tag{21}$$

The transverse shear strain in the equivalent homogenized shell is assumed to be the weighted average of the strains in the faces and core as follows:

$$\begin{aligned}
h_t d\epsilon_{yz}^e &= 2h_f d\epsilon_{yz}^f + h_c d\epsilon_{yz}^c \\
h_t d\epsilon_{xz}^e &= 2h_f d\epsilon_{xz}^f + h_c d\epsilon_{xz}^c
\end{aligned} \tag{22}$$

Using the above equations (21 and 22), the transverse shear stresses in the equivalent homogenized shell can be obtained as follows:

$$\begin{aligned}
d\sigma_{yz}^e &= \frac{h_t d\epsilon_{yz}^e}{\frac{2h_f}{C_{55}^f} + \frac{h_c}{C_{55}^c}} \\
d\sigma_{xz}^e &= \frac{h_t d\epsilon_{xz}^e}{\frac{2h_f}{C_{66}^f} + \frac{h_c}{C_{66}^c}}
\end{aligned} \tag{23}$$

Based on the above-described algorithm, a new sandwich material model is defined within the DYNA3D nonlinear FE code. The only change that had to be made outside the material model definition is the way the through thickness integration is performed in the Hughes shell element. Instead of performing the integration on a point-wise basis, the strains for all integration points together with the integration points z -coordinates have to be gathered and passed to the sandwich material model. An important advantage of the approach is that the constitutive sandwich material subroutine is called only once for the whole cross section, while for a homogeneous shell the corresponding constitutive subroutine has to be called once for each through thickness integration point.

VALIDATION OF THE SOLUTION METHODOLOGY

To assess the performance of the developed methodology, two models are investigated. 3-D FE numerical solutions can be obtained for the first model and experimental data is available for the second model. The first model considered is a sandwich plate with Aluminum faces and Foam core. The sandwich plate is tested by Bau-Madsen [5] for several different lateral pressures (see Figure 3). A convergent 2-D finite element mesh of the plate is development and the current formulation is employed for the simulation. Figure (4) depicts the predicted center deflection, for several lateral pressures, for two boundary conditions. An excellent agreement with the experimental data is obtained for both boundary conditions. The second model considered is a symmetric sandwich beam; 300 mm in length, 5 mm in width, and consisting of 1 mm Aluminum faces and 16 mm PVC Foam core. Material constants for the model are reported in Table (1). Due to symmetry, only one half the beam is modeled. The beam is modeled both by 3-D brick elements and the developed sandwich shell element as depicted by Figures (5) and (6) respectively. The 3-D model consists of two elements for each face and four elements for the core through the thickness. Thirty elements are considered along the beam length defining a mesh of 30x8x1 brick elements. The sandwich shell is modeled by 30x1 mesh. The utilized mesh in here is obtained after mesh convergent studies. The implementation of the methodology into the explicit dynamic finite element code DYNA3D requires definition of the density of the sandwich shell. The density of the sandwich shell is assumed to be the weighted average of the densities of the core and faces as given by the following equation:

$$\rho^e = \frac{2h_f \rho^f + h_c \rho^c}{h_t} \tag{24}$$

where ρ^e , ρ^f , ρ^c are the densities for the equivalent shell, faces, and core respectively.

Figure (7) depicts the FE model of the 3-D sandwich beam with coordinate axes, direction of load, and stations at which strains are extracted for comparison. The commercial explicit code LSDYNA [6,7] and the implicit code ABAQUS are used to assess the accuracy of the developed methodology.

The center deflection of the 3-D sandwich beam is 8.4 mm as compared to a predicted value of 8.5 mm utilizing the current formulation. The lateral pressure of 1.5 N/mm² is applied to the sandwich beam. Results for the normal strains, ϵ_{xx} , are presented in Figures (8), (9), and (10) at different locations of the sandwich beam. In the central region of the beam where warping is insignificant, the present approach yields excellent results as compared with the 3-D models. As warping become significant, the strain distributions using the presented approach become less accurate due to the constraint of linear in-plane strain distribution of the utilized Mindlin theory in the shell formulation. In addition, the clamped boundary condition in the shell elements is not the same as that of the 3-D elements. Figures (11) and (12) depict the distribution of the transverse shear strain, ϵ_{xz} , at two different locations of the beam. In here, a very good agreement of the transverse shear strain between the developed formulation and the 3-D model is obtained. Figure (13) depicts the normal stress, σ_{xx} , at center of beam. Good agreement is also obtained for the stress.

Table 1. Properties for face and core

	E ₁₁ GPa	E ₂₂ GPa	E ₃₃ GPa	v ₁₂	v ₃₁	v ₃₂	G ₁₂ GPa	G ₃₁ GPa	G ₃₂ GPa	ρ kg/m ³
Face: Alum	73.4	73.4	73.4	0.32	0.32	0.32	27.8	27.8	27.8	2700
Core: PVC Foam	0.286	0.286	0.286	0.3	0.3	0.3	0.11	0.11	0.11	250

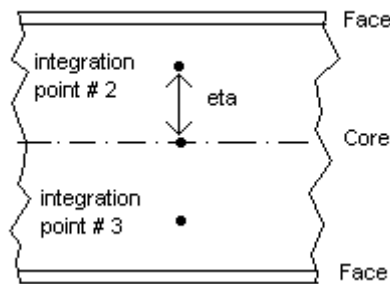


Figure 1. Integration points through the thickness of the shell

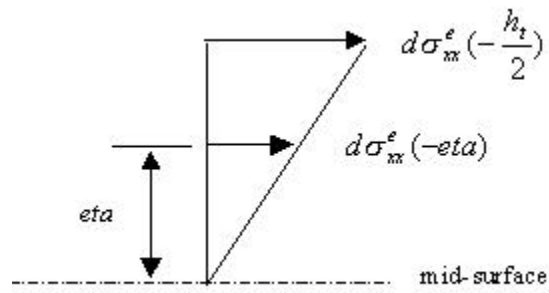


Figure 2. Equivalent stress at the surface and integration point #2 of the shell

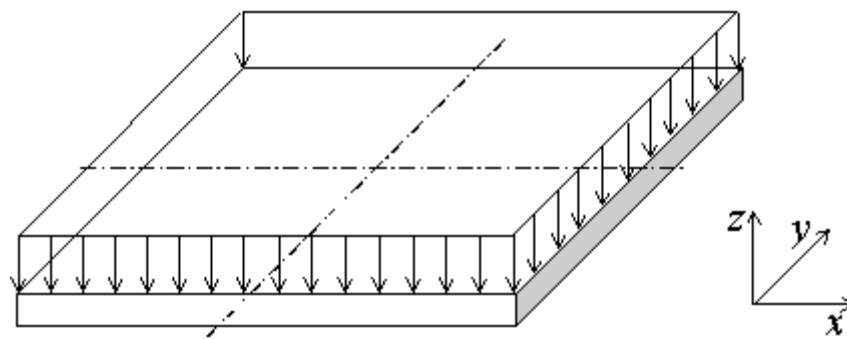


Figure 3. Sandwich plate geometry from experimental testing of Bau-Madsen ⁸

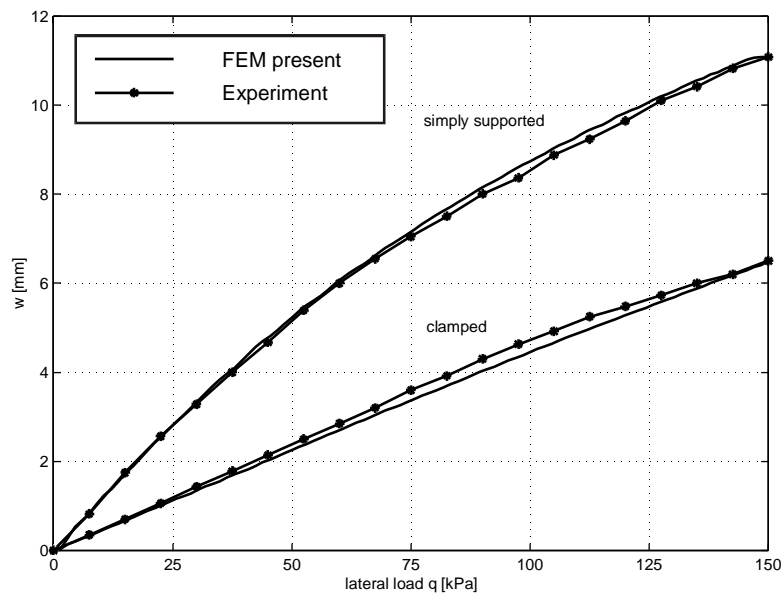


Figure 4. Displacement, w , at midpoint of the sandwich plate for lateral pressure $q = 0 \div 150$ kPa, for clamped and simply supported plate (models of ⁸)

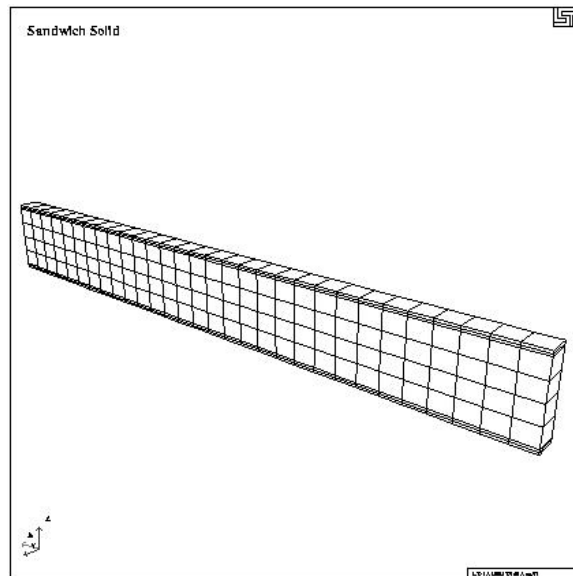


Figure 5. Brick FE model of one half of the structure

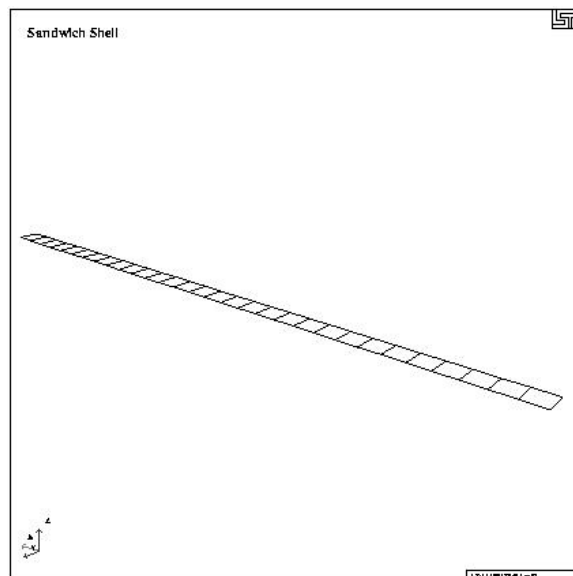


Figure 6. Shell FE model of one half of the structure

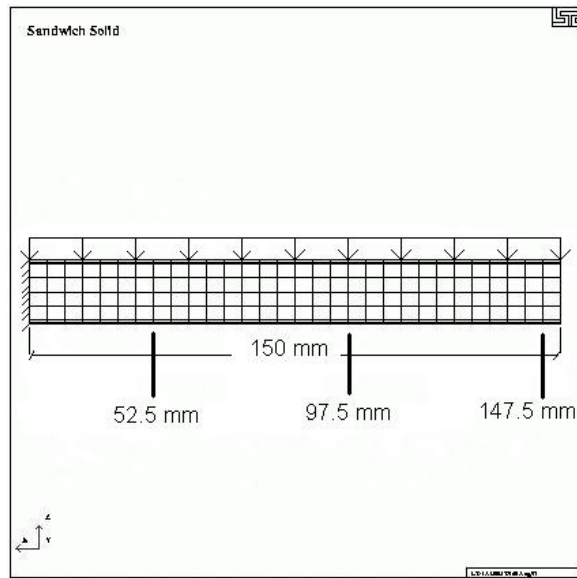


Figure 7. Geometry and locations of sections for strain extraction

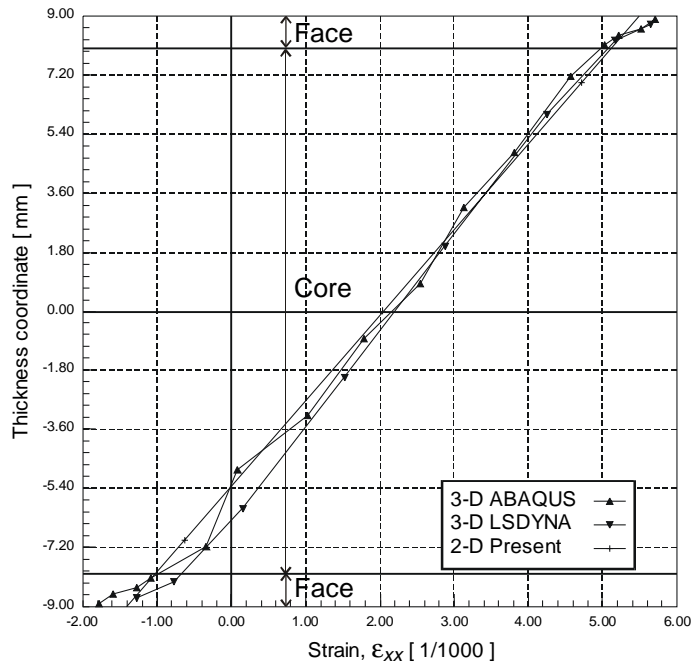


Figure 8. Normal Strains, ϵ_{xx} , in the Midsection ($x = 147.5$ mm)

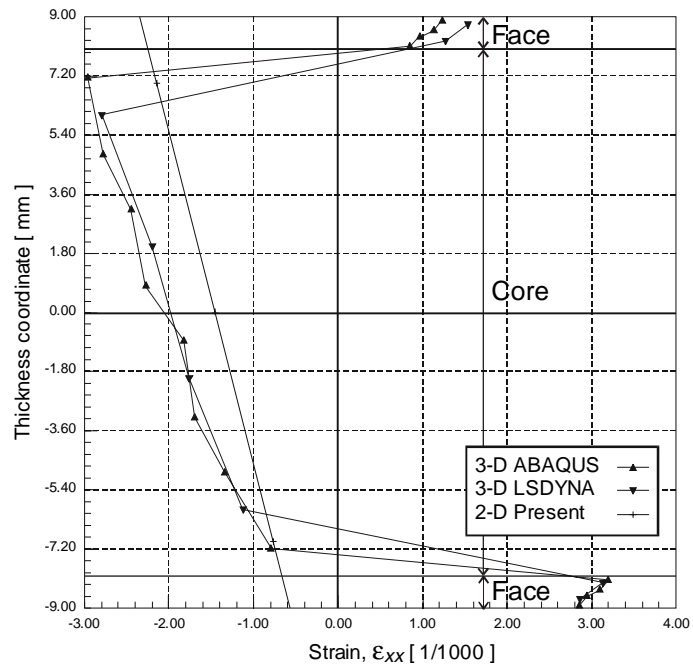


Figure 9. Normal Strains, ϵ_{xx} , at $x = 52.5$ mm

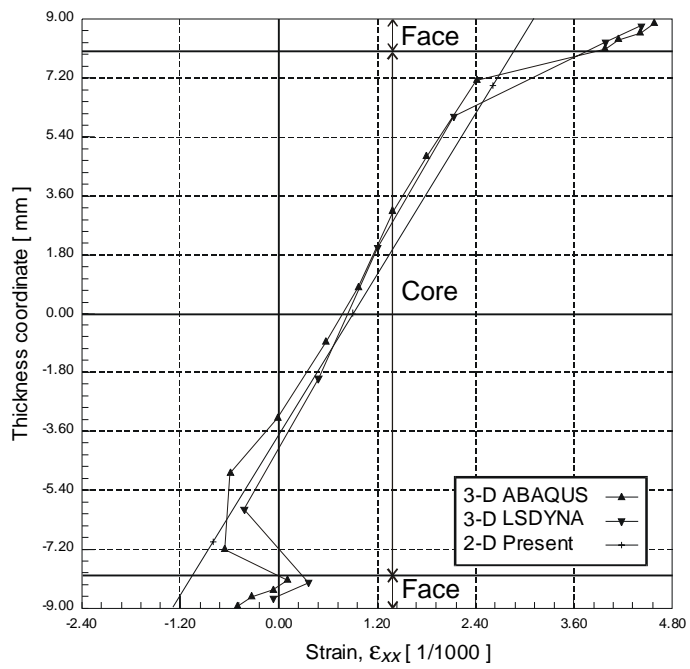


Figure 10. Normal Strains, ϵ_{xx} , at $x = 97.5$ mm

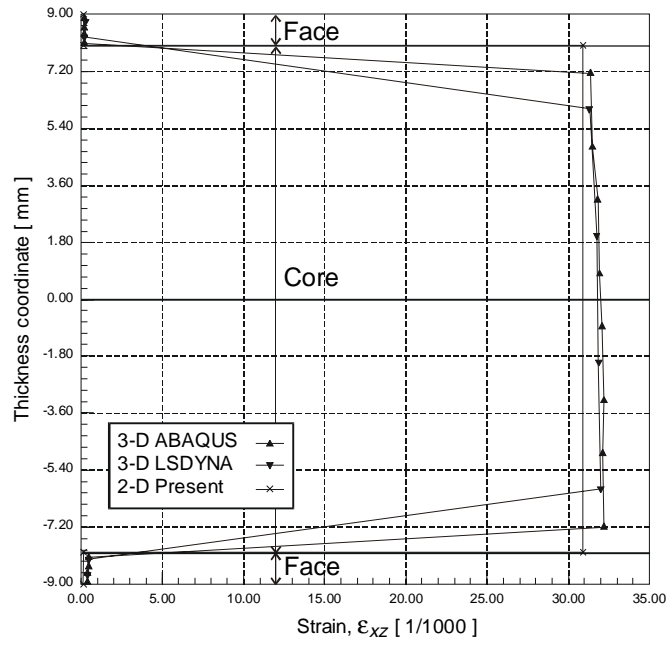


Figure 11. Shear Strains, ϵ_{xz} , at $x = 52.5$ mm

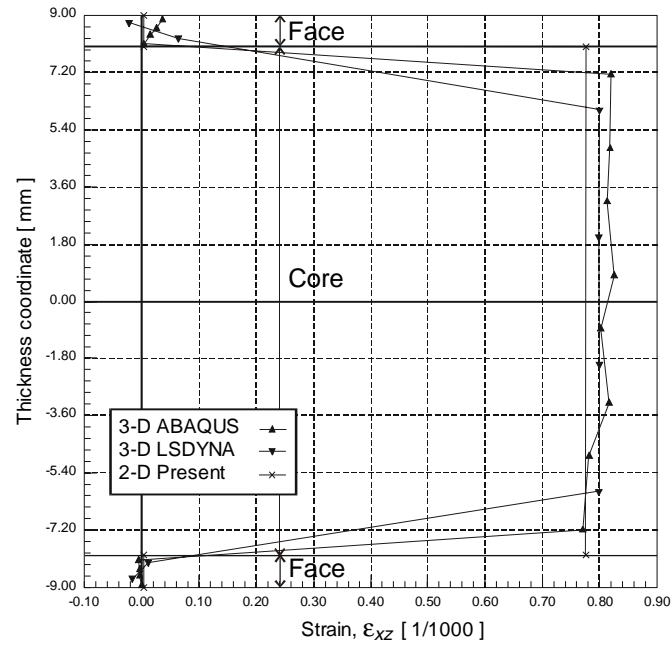


Figure 12. Shear Strains, ϵ_{xz} , at $x = 147.5$ mm

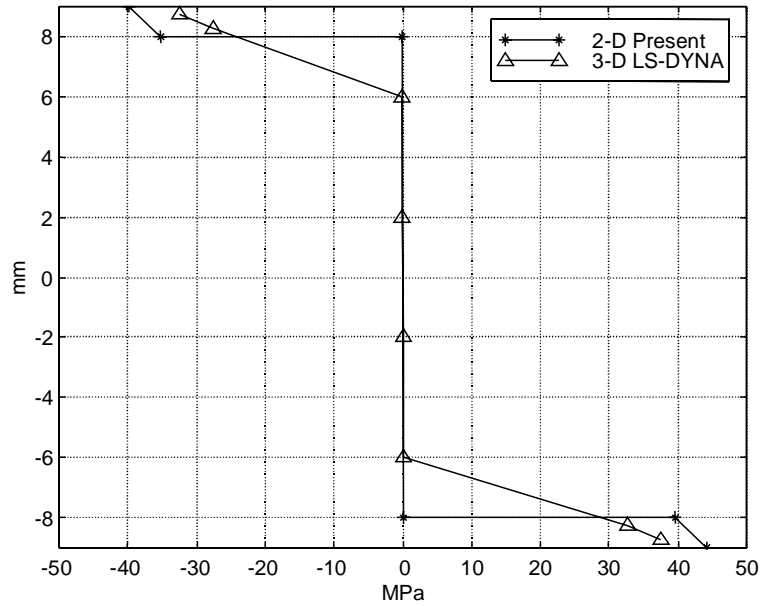


Figure 13. Normal stress, σ_{xx} , at $x = 147.5$ mm

CONCLUSIONS

The sandwich homogenization procedure herein presented can be easily and efficiently implemented into standard FE codes. The procedure can be combined with existing shell elements for homogeneous shells to produce a powerful analysis tool able to analyze both simple and complicated sandwich structures. The present implementation of the SHOP involves the simplest shear deformable elements yet it provides excellent results for the transverse shear strains and stresses, the normal strains and stresses in regions without excessive warping, and the overall shell behavior. The computational efficiency of the present analysis is comparable with the most efficient formulations for homogeneous orthotropic shells. The general approach that the SHOP is based upon could have great potential when combined with a higher order shell formulation.

ACKNOWLEDGEMENTS

The research within this study was supported by grant F49620-98-1-0384 from the Airforce Office of Scientific Research. Computing support is provided by the Ohio Supercomputer Center. The support is gratefully acknowledged. The authors would like to extend sincere thanks to the Lawrence Livermore National Laboratory (LLNL) for providing the source codes for DYNA3D.

REFERENCES

1. E. Reissner, "Finite Deflections of Sandwich Plates", *Journal of Aeronautical Science*, **15** (7), 435–440 (1948).

2. R. D. Mindlin, "Influence of Rotary Inertia and Shear on Flexural Motions of Isotropic, Elastic Plates", *Journal of Applied Mechanics, Transactions of the ASME*, **18**, 31–38 (1951).
3. M. M. Hrabok and T. M. Hrudý, "A Review and Catalogue of Plate Bending Finite Elements", *Computers & Structures*, **19** (3), 479–495 (1984).
4. K. H. Ha, "Finite Element Analysis of Sandwich Plates: An Overview", *Computers & Structures*, **37** (4), 397–403 (1990).
5. W. S. Burton and A. K. Noor, "Assessment of Computational Models for Sandwich Panels and Shells", *Computer Methods in Applied Mechanics and Engineering*, **124** (1–2), 125–151 (1995).
6. D. Zenkert, *An Introduction to Sandwich Construction*, Chameleon Press, London, 1995.
7. A. K. Noor, W. S. Burton and C. W. Bert, "Computational Models for Sandwich Panels and Shells", *Applied Mechanics Reviews*, **49** (3), 155–199 (1996).
8. B. N. Pandya and T. Kant, "Higher-Order Shear Deformable Theories for Flexure of Sandwich Plates – Finite Element Evaluations", *International Journal of Solids and Structures*, **24** (12), 1267–1286 (1988).
9. J. N. Reddy, "A Review of Refined Theories Laminated Composite Plates", *The Shock and Vibration Digest*, **22** (7), 3–17 (1990).
10. T. Kant and J. R. Kommineni, "Geometrically Non-Linear Transient Analysis of Laminated Composite and Sandwich Shells with a Refined Theory and C^0 Finite Elements", *Computers & Structures*, **52** (6), 1243–1259 (1994).
11. A. Toledano and H. Murakami, "A Composite Plate Theory for Arbitrary Laminate Configuration", *Journal of Applied Mechanics*, **54** (1), 181–189 (1987).
12. X. Lu and D. Liu, "Interlaminar Shear Stress Continuity Theory for Both Thin and Thick Composite Laminates", *Journal of Applied Mechanics*, **59** (3), 502–509 (1992).
13. C. Y. Lee and D. Liu, "An Interlaminar Stress Continuity Theory for Laminate Composite Analysis", *Computers & Structures*, **42** (1), 69–78 (1992).
14. Y. Frostig and M. Baruch, "High-Order Bending of Sandwich Panels with a Transversely Flexible Core", *Collection of Technical Papers – Proceedings of the 35-th AIAA/ASME/ASCE/AHS/ASC Structures, Structural Dynamics, and Materials Conference*, AIAA, New York, NY, USA, **2**, 721–735 (1994).
15. S. Oskooei and J. S. Hansen, "A Higher Order Finite Element for Sandwich Plates", *Collection of Technical Papers – Proceedings of the 39-th AIAA/ASME/ASCE/AHS Structures, Structural Dynamics and Materials Conference*, AIAA, New York, NY, USA, **1**, 147–156 (1998).
16. M. DiSciuva, "A General Quadrilateral Multilayered Plate Element with Continuous Interlaminar Stresses", *Computers & Structures*, **47** (1), 91–105 (1993).
17. M. Cho and R. R. Parmerter, "Efficient Higher Order Composite Plate Theory for General Lamination Configurations", *AIAA Journal*, **31** (7), 1299–1306 (1993).
18. Y. B. Cho and R. C. Averill, "An Improved Theory and Finite-Element Model for Laminated Composite and Sandwich Beams Using First-Order Zig-Zag Sublaminar Approximations", *Composite Structures*, **37** (3/4), 281–298 (1997).
19. Y. B. Cho, E. J. Plaskacz, R. C. Averill and R. F. Kulak, "Explicit Dynamic Finite Element Analysis of Laminated Composite Automotive Structures Using a New Composite Plate Element", *Crashworthiness, Occupant Protection and Biomechanics in Transportation Systems*, ASME, AMD-Vol. 225/BED-Vol. 38, ASME, Fairfield, HJ, USA, 73–107 (1997).
20. Hughes T. JR. and Liu W. K., "Nonlinear Finite Element Analysis of Shells: Part II. Three Dimensional Shells", *Computer Methods in Applied Mechanics*, Vol. 27, pp. 331–362, 1981.